Manuscript prepared for Geosci. Model Dev.
with version 2014/07/29 7.12 Copernicus papers of the LaTeX class copernicus.cls.
Date: 7 June 2016

# OMEN-SED 1.0: A new, numerically efficient sediment module for the coupling to Earth System Models

Dominik Hülse[1], Sandra Arndt[1], Stuart Daines[2], and Andy Ridgwell[1, 3]

[1]School of Geographical Sciences, University of Bristol, Clifton, Bristol BS8 1SS, UK
[2]Earth System Science, University of Exeter, North Park Road, Exeter EX4 4QE, UK
[3]Department of Earth Sciences, University of California, Riverside, CA 92521, USA

*Correspondence to:* Sandra Arndt (s.arndt@bristol.ac.uk)

**Abstract.** Here we describe the first version of the OrganicMatter ENabled SEDiment model (OMEN-SED 1.0).

## 1 Introduction

Degradation of organic matter (OM) in marine sediments fuels benthic biogeochemical processes and the resulting fluxes across the sediment-water interface are of considerable importance for many global biogeochemical cycles (Arndt et al., 2013). Burial of OM represents an important connection between carbon stored in more climate-relevant reservoirs like the oceans, atmosphere, and the marine sediments and carbon that is sequestered for much longer, geological timescales in sedimentary rock or coal (Mackenzie, 2005; Burdige, 2007). Biological primary production of organic matter ($CH_2O$ in equation R1) and the reverse process of degradation can be written in a greatly simplified reaction as:

$$CO_2 + H_2O \rightleftharpoons CH_2O + O_2. \quad \text{(R1)}$$

On long timescales production of OM is generally greater than degradation which results in some organic matter being buried in marine sediments and oxygen accumulating in the atmosphere. Thus burial of OM leads to net oxygen input to, and $CO_2$ removal from, the atmosphere (Berner, 2004). Therefore, globally quantifying the degradation of organic matter in marine sediments and related biogeochemical dynamics is important for understanding climate and the cycling of many chemical elements on various timescales. Such studies and quantifications are possible through the application of idealised mathematical representations of diagenesis, or so-called diagenetic models (e.g. Berner, 1980; Boudreau, 1997). The number of research questions that can be addressed with diagenetic

models is infinite and a plethora of different approaches have been developed, mainly following two distinct directions (Arndt et al., 2013). First, state-of-the art diagenetic models simulating all of the essential coupled redox and equilibrium reactions within marine sediments that control carbon burial and benthic recycling fluxes (e.g. BRNS, Aguilera et al., 2005; MEDIA, Meysman et al., 2003; OMEXDIA, Soetaert et al., 1996b). These "complete" models generally use a so-called multi-G approach, thus dividing the bulk organic carbon pool into a number of compound classes that are characterised by different degradabilities $k_i$. However, their global applicability is limited by the high computation cost of simulating all biogeochemical reactions. The second group of models is less sophisticated and comprehensive than the "complete" diagenetic models and is used for the coupling to global Earth System Models (e.g. DCESS, Shaffer et al., 2008; HAMOCC, , Heinze et al., 1999; MEDUSA, Munhoven, 2007). In particular, these models consider fewer biogeochemical reactions and apply the 1G approach, thus just representing a single organic matter pool which is degraded at a constant rate.

TODO: Sandra review: large scale of published model parameters illustrates the complex nature of organic matter dynamics! Very difficult to find global relationships to relate model parameters to available environmental characteristics, such as water depth, deposition rate. Sentence about: even though there is some potential most ESM use the following:

In most current Earth System models, sediment-water exchange of OM and chemical elements is generally treated in a very simplistic way (Soetaert et al., 2000; Hülse et al., 2016). Most Earth system Models of Intermediate Complexity (EMICs) for instance represent the sediment-water interface either as a reflective or a conservative/semi-reflective boundary (Hülse et al., 2016). Thus, all particulate material deposited on the seafloor is either instantaneously consumed (reflective boundary), or a fixed fraction is buried in the sediments (conservative/semi-reflective boundary). Both highly simplified approaches furthermore completely neglect the exchange of solute species through the sediment-water interface and, therefore, cannot resolve the complex benthic-pelagic coupling. However, due to their computational efficiency, both representations are often used in global biogeochemical models (e.g. Najjar et al., 2007; Ridgwell et al., 2007; Goosse et al., 2010)

See e.g. (Soetaert et al., 2000; Mackenzie et al., 2004).

How are sediment resolved in Earth System models

See e.g. (Soetaert et al., 2000)

Problem with that:

The spatial variability in e.g. benthic particulate organic carbon (POC) mineralization kinetics throughout the ocean is currently unknown. This creates considerable uncertainties when diagenetic models are used to couple benthic and pelagic biogeochemical cycles in global models. (Kriest and Oschlies, 2011)

Alternative Model approaches, e.g. from coastal research

Here, we present the OrganicMatter ENabled SEDiment model (OMEN-SED 1.0), a new, one-dimensional, numerically efficient reactive transport model (RTM) for the biogeochemical dynamics of organic matter, related chemical elements (O, N, S, P) and associated pore water quantities (ALK, DIC) in deep-sea sediments. OMEN-SEDs computational efficiency makes it appropriate for the coupling to Earth System Models and therefore for studying global biogeochemical dynamics over geological timescales. Also mention here presented as a 2G-Model, however OMEN-SED can easily be extended to a Multi-G approach.

See Van Cappellen and Wang (1996): "Metal cycling in surface sediments: Modeling the interplay or transport and reaction" for some good basic info!

## 2 Model Description

This section describes the formulation and solution of the model (see Table 1 for the implemented processes). A glossary of parameters along with their respective units is provided in Tables 6 and 7.

### 2.1 General Model Approach

The calculation of benthic return/uptake and burial fluxes is based on the vertically resolved conservation equation for solid and dissolved species in porous media is given by (e.g. Berner, 1980; Boudreau, 1997):

$$\frac{\partial \xi C_i}{\partial t} = -\frac{\partial F}{\partial z} + \xi \sum_j R_i^j \tag{1}$$

where $C_i$ is the concentration of the biogeochemical species $i$, $\xi$ equals the porosity $\phi$ for solute species and $(1-\phi)$ for solid species, hence represents the partitioning of species $i$ into the solute and dissolved phase. The term $z$ is the sediment depth, $t$ denotes the time, $F$ summarises the transport fluxes and $\sum_j R_i^j$ represents the sum of production/consumption rates $j$ that affect species $i$. The reaction network has to account for the most important primary and secondary redox reactions, equilibrium reactions, mineral dissolution and precipitation, as well as adsorption and desorption processes.

State-of-the-art reaction-transport models generally solve the ordinary differential equation (ODE) (1) numerically and thus allow to account for transient conditions, depth-varying parameters or a high degree of coupling between different chemical species. Yet, numerical models are computa-

tional expensive, thus rendering their application in an Earth System Model framework prohibitive. An analytical solution of Eq. (1) provides an alternative and computational more efficient approach. Analytical models enjoyed great popularity in the early days of diagenetic modelling due to the low computing power. However, early analytical models were often very problem-specific and only considered one or two coupled species (e.g. Lehrman, Berner) ?? which pubs?. A number of more complex analytical models describing the coupled dynamics of ....were developed (e.g. Billen, 1982; Goloway and Bender, 1982; Jahnke et al., 1982).

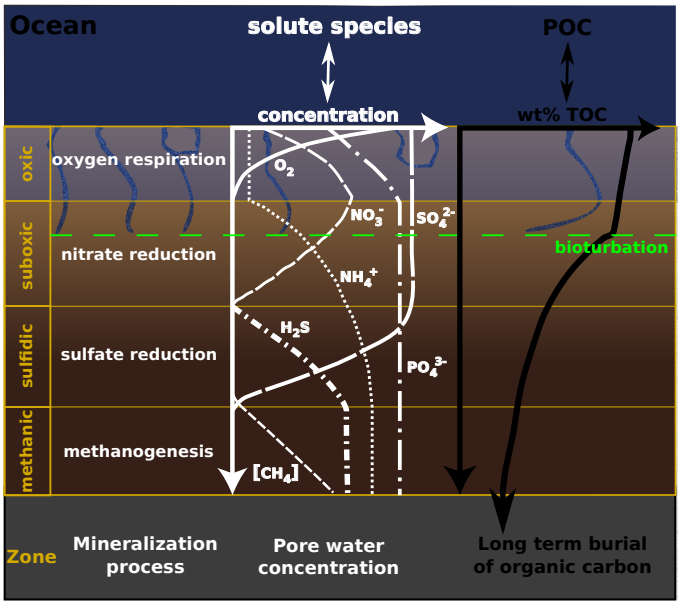


**Figure 1.** Schematic of the different modelled species and layers in our sediment model. Here showing the case $z_{\mathrm{ox}} < z_{\mathrm{bio}} < z_{\mathrm{NO_3}} < z_{\mathrm{SO_4}}$.

Finding an analytical solution to Eq. (1), especially when complex reaction networks are to be considered is not straightforward and generally requires the assumption of steady state. Because the Earth system model relevant variability in boundary conditions and fluxes is generally longer than the characteristic timescales of the reaction-transport processes, the sediment can be described by a series of pseudo steady-states. In addition, the complexity of the reaction network can be reduced by dividing the sediment into distinct zones and accounting for the most pertinent biogeochemical processes within each zone, thus increasing the likelihood of finding an analytical solution to Eq. (1). The model divides the sediment into a bioturbated and a non-bioturbated zone defined by the constant bioturbation depth $z_{\mathrm{bio}}$. In addition, it accounts for the dynamic redox zonation of marine sediments by dividing the sediment into: 2) an oxic zone situated between the SWI and a dynamically calculated penetration depth of oxygen $z_{\mathrm{ox}}$, 3) a denitrification zone situated between $z_{\mathrm{ox}}$ and a dynamically calculated penetration depth of nitrate $z_{\mathrm{NO_3}}$, 4) a sulfate reduction zone situated between $z_{\mathrm{NO_3}}$ and

a dynamically calculated penetration depth of sulfate $z_{SO_4}$ and 5) a methanic zone situated below $z_{SO_4}$ (Figure 1). Each zone is characterised by a set of diagenetic equations that encapsulate the most pertinent reaction and transport processes in the respective zone (see section 2.2 and 2.3 for more details).

OMEN calculates and feeds back to the Earth System model the fraction of POC preserved in the sediments and the sediment-water interface fluxes of the dissolved species $C_i$:

$$\text{Flux\_SWI}(\text{C}_\text{i}) = \phi \cdot \left( D_i \frac{\partial C_i}{\partial z} + w C_i(0) \right) \tag{2}$$

where $w$ is the deposition rate, $D_i$ is the diffusion coefficient and $C_i(0)$ the sediment-water concentration of species $i$.

### 2.2 Transport

The model accounts for both advection and diffusion of dissolved and solid species, assuming that sediment compaction is negligible ($\frac{\partial \phi}{\partial z}$=0). The diffusion of dissolved species is described via an apparent diffusion coefficient, $D_{i0}$. In addition, the activity of infaunal organisms in the bioturbated zone of the sediment ($z < z_{\text{bio}}$) causes random displacements of sediments and porewaters and is simulated using a diffusive term (e.g. Boudreau,1986), with a constant bioturbation coefficient $D_{\text{bio}}$ in the bioturbated zone. The pumping activity by burrow-dwelling animals and the resulting ventilation of tubes, the so-called bioirrigation, is encapsulated in a factor, $f_{ir}$ that enhances the molecular diffusion coefficient, $D_{\text{mol},i}$ ( hence, $D_{i,0} = D_{\text{mol},i} \cdot f_{ir}$, Soetaert et al., 1996a). The divergence of the flux is thus given by:

$$\frac{\partial F}{\partial z} = -\frac{\partial}{\partial z} \left( -\xi D_i \frac{\partial C_i}{\partial z} + \xi w C_i \right) \tag{3}$$

where $D_i$ is the diffusion coefficient of species $i$ ($D_i = D_{i,0} + D_{\text{bio}} = D_{\text{mol},i} \cdot f_{ir} + D_{\text{bio}}$ for dissolved species and $D_i = D_{\text{bio}}$ for solid species) and $w$ is the deposition rate. The bioturbation coefficient $D_{\text{bio}}$ is set to zero below $z_{\text{bio}}$. In addition, infaunnal activity ceases ($D_{\text{bio}} = 0$) once bottom waters become anoxic ($O_2$ = 0.0 mol cm$^{-3}$ ). add if-query in code!!

### 2.3 Reaction Network

Earth System models generally track the evolution of the global biogeochemical cycles of organic and inorganic carbon, the essential nutrients (nitrogen, phosphorus) and oxygen with the aim of investigating the evolution of the ocean's redox structure and carbonate system and its feedbacks on global climate. This general aim thus defines a minimum set of state variables and reaction processes that need to be resolved for an efficient representation of the benthic-pelagic coupling in Earth System Models. The sediment model has to provide robust quantifications of organic and inorganic carbon burial fluxes, growth-limiting nutrient, equilibrium invariant and reduced species return fluxes, and oxygen uptake fluxes. As a consequence, the reaction network must explicitly or implicitly account for the most important primary and secondary redox reactions, equilibrium reactions, mineral

**Table 1.** Reactions and variables implemented in the Reaction Network of OMEN-SED (1.0). The primary and secondary redox reactions are listed in the sequence they occur with increasing sediment depth.

| | Description |
|---|---|
| Primary redox reactions | Degradation of organic matter via aerobic respiration, denitrification, sulfate reduction, methanogenesis (implicit) |
| Secondary redox reactions | Oxidation of ammonium and sulfide by oxygen, anaerobic oxidation of methane by sulfate |
| Adsorption/Desorption | Ad-/Desorption of P on/from $\mathrm{Fe(OH)_3}$, $\mathrm{NH_4}$ adsorption, $\mathrm{PO_4}$ adsorption |
| Mineral precipitation | Formation of authigenic P |
| Variables | Organic matter, oxygen, nitrate, ammonium, sulfate, sulfide (hydrogen sulfide), phosphate, Fe-bound P, DIC, ALK |

precipitation/dissolution and adsorption/desorption, resulting in a complex set of coupled reaction-transport equations. The following subsections provide a short discussion of the reaction processes included in the model and give an overview of the vertically resolved conservation equations and boundary conditions for solid and dissolved species in each layer. Table 1 states the reactions and variables considered in the reaction network.

### 2.3.1 Organic matter

In marine sediments, organic matter (OM) is degraded by heterotrophic activity coupled to the sequential utilisation of terminal electron acceptors (TEAs), typically in the order of $\mathrm{O_2}$, $\mathrm{NO_3^-}$, Mn(VI), Fe(III) and $\mathrm{SO_4^{2-}}$ followed by methanogenesis and/or fermentation. Organic matter degradation is described via a multi-G model approach (Arndt et al., 2013, and references therein), assuming that the bulk OM is divided into discrete compound classes $C_i$ characterised by specific degradation rate constants $k_i$. Such a multi-G approach allows for selective preservation of compound classes according to their degradability, $k_i$ and, thus, accounts for the change in organic matter degradability with burial. Each compound class is degraded according to first-order kinetics. Organic matter dynamics are thus described by:

$$\frac{\partial C_i}{\partial t} = 0 = D_{C_i}\frac{\partial^2 C_i}{\partial z^2} - w\frac{\partial C_i}{\partial z} - k_i \cdot C_i \tag{4}$$

The solution of Eq. 4 (see section **??** for details) requires the definition of boundary conditions. The model assumes a known concentration/flux at the sediment-water interface and continuity across the bottom of the bioturbated zone, $z_{\mathrm{bio}}$ (Table 2).

**Table 2.** Boundary conditions for organic matter and oxygen.

| Boundary | Condition | |
|---|---|---|
| $z = 0$ | known concentration | 1) $C_i(0) = C_{i0}$ |
| $z = z_{\mathrm{bio}}$ | continuity | 2) $C_i(z_{\mathrm{bio}}^-)$=$C_i(z_{\mathrm{bio}}^+)$ |
| | | 3) $-D_{\mathrm{bio}} \cdot \frac{\partial C_i}{\partial z}\vert_{z_{\mathrm{bio}}^-} = 0$ |
| $z = 0$ | known concentration | 1) $\mathrm{O_2}(0) = O_{20}$ |
| $z = z_{\mathrm{bio}}$ | continuity | 2) $\mathrm{O_2}(z_{\mathrm{bio}}^-)$=$\mathrm{O_2}(z_{\mathrm{bio}}^+)$ |
| | | 3) $-(D_{\mathrm{O_2},0} + D_{\mathrm{bio}}) \cdot \frac{\partial \mathrm{O_2}}{\partial z}\vert_{z_{\mathrm{bio}}^-} = -D_{\mathrm{O_2},0} \cdot \frac{\partial \mathrm{O_2}}{\partial z}\vert_{z_{\mathrm{bio}}^+}$ |
| $z = z_{\mathrm{ox}}$ | $\mathrm{O_2}$ consumption | 4) **IF** $(\mathrm{O_2}(z_\infty) > 0)$ |
| | $(z_{\mathrm{ox}} = z_\infty)$ | $\frac{\partial \mathrm{O_2}}{\partial z}\vert_{z_{\mathrm{ox}}} = 0$ |
| | | **ELSE** |
| | $(z_{\mathrm{ox}} < z_\infty)$ | $\mathrm{O_2}(z_{\mathrm{ox}}) = 0$ and $-D_{\mathrm{O_2}} \cdot \frac{\partial \mathrm{O_2}}{\partial z}\vert_{z_{\mathrm{ox}}} = F_{red}(z_{\mathrm{ox}})$ |
| | with flux from below | $F_{red}(z_{\mathrm{ox}}) = \frac{1-\phi}{\phi} \cdot \int_{z_{\mathrm{ox}}}^{\infty} \sum_i (2\gamma_{\mathrm{NH_4}}\mathrm{NC_i} + \gamma_{\mathrm{H_2S}}\mathrm{SO_4C})\, k_i C_i \, dz$ |

### 2.3.2 Oxygen

Oxygen serves as the most powerful terminal electron acceptor for the heterotrophic degradation of organic carbon. In addition, the oxidation of reduced species produced through microbial activity throughout the sediment column further contributes to the consumption of oxygen. The model explicitly accounts for the consumption of oxygen by heterotrophic degradation and nitrification of ammonium in the oxic layer of the sediment. The nitrification of 1 mol of ammonium in the oxic layer consumes 2 mol of oxygen. In addition, the oxygen consumption through the oxidation of reduced species ($\mathrm{Fe^{2+}}$, $\mathrm{Mn^{2+}}$, $\mathrm{NH_4}$, $\mathrm{H_2S}$) produced in the suboxic and anoxic layers of the sediment is implicitly taken into account through the flux boundary condition at the dynamic oxygen penetration depth $z_{\mathrm{ox}}$. This simplification can be justified as it has been shown that these secondary redox reactions mainly occur at the oxic/suboxic interface (Soetaert et al., 1996b). Oxygen is described in $\mathrm{mol\,cm^{-3}}$ liquid and conversion from the solid phase of mineralized organic matter (expressed in $\mathrm{mol\,cm^{-3}}$ bulk sediment) to consumption of dissolved oxygen (or later nutrients) introduce a factor of $\frac{1-\phi}{\phi}$, where $\phi$ is the sediment porosity. Oxygen dynamics are thus described by:

$$\frac{\partial \mathrm{O_2}}{\partial t} = 0 = D_{\mathrm{O_2}} \frac{\partial^2 \mathrm{O_2}}{\partial z^2} - w \frac{\partial \mathrm{O_2}}{\partial z} - \frac{1-\phi}{\phi} \sum_i k_i \cdot [OC + 2\gamma_{\mathrm{NH_4}}\mathrm{NC_i}] \cdot C_i(z) \tag{5}$$

To solve Eq. 5 analytically (see section **??**) boundary conditions at three depths are defined (Table 2). The model assumes a known bottom water concentration and the complete consumption of oxygen at the oxygen penetration depth (or zero flux if $z_{\mathrm{ox}} = z_\infty$). It considers equal oxygen concentration and diffusive flux above ($z_{\mathrm{bio}}^-$) and below ($z_{\mathrm{bio}}^+$) the bioturbation boundary. In addition, the model imposes a flux of reduced species through the bottom of the oxic zone that is calculated as the reduced

substances produced through anoxic mineralization of organic matter below $z_{\mathrm{ox}}$. Thus, assuming that fractions ($\gamma_{\mathrm{NH_4}}$ and $\delta$) of these reduced species are oxidised at the oxic/suboxic interface.

### 2.3.3 Nitrate and Ammonium

To model nitrate and ammonium dynamics the sediment is partitioned into two geochemical layers (oxic and suboxic), where different equations describe the biogeochemical processes. Above the oxygen penetration depth organic matter mineralization produces ammonium, which is partly nitrified to nitrate (the fraction $\gamma_{\mathrm{NH_4}}$). In the suboxic zone ($z > z_{\mathrm{ox}}$), oxygen concentration is zero and nitrate serves as the electron acceptor to respire organic matter, thus nitrate is consumed by denitrification and ammonium is produced. Below the nitrate penetration depth $z_{\mathrm{NO_3}}$, ammonium is still produced through OM mineralization. Therefore the diagenetic equations for nitrate and ammonium are given by:

1. Layer ($z \leq z_{\mathrm{ox}}$)

$$\frac{\partial NO_3^I}{\partial t} = 0 = D_{NO_3}\frac{\partial^2 NO_3^I}{\partial z^2} - w\frac{\partial NO_3^I}{\partial z} + \gamma_{\mathrm{NH_4}}\frac{1-\phi}{\phi}\cdot\sum_i \mathrm{NC_i}\cdot k_i\cdot C_i(z) \tag{6}$$

$$\frac{\partial \mathrm{NH_4}^I}{\partial t} = 0 = \frac{D_{\mathrm{NH_4}}}{1+K_{\mathrm{NH_4}}}\frac{\partial^2 \mathrm{NH_4}^I}{\partial z^2} - w\frac{\partial \mathrm{NH_4}^I}{\partial z} + \frac{1-\gamma_{\mathrm{NH_4}}}{1+K_{\mathrm{NH_4}}}\cdot\frac{1-\phi}{\phi}\cdot\sum_i \mathrm{NC_i}\cdot k_i\cdot C_i(z) \tag{7}$$

2. Layer ($z_{\mathrm{ox}} < z \leq z_{\mathrm{NO_3}}$)

$$\frac{\partial NO_3^{II}}{\partial t} = 0 = D_{NO_3}\frac{\partial^2 NO_3^{II}}{\partial z^2} - w\frac{\partial NO_3^{II}}{\partial z} - \frac{1-\phi}{\phi}NO_3C\cdot\sum_i k_i\cdot C_i(z) \tag{8}$$

$$\frac{\partial \mathrm{NH_4}^{II}}{\partial t} = 0 = \frac{D_{\mathrm{NH_4}}}{1+K_{\mathrm{NH_4}}}\frac{\partial^2 \mathrm{NH_4}^{II}}{\partial z^2} - w\frac{\partial \mathrm{NH_4}^{II}}{\partial z} \tag{9}$$

3. Layer ($z_{\mathrm{NO_3}} < z \leq z_{\infty}$)

$$\frac{\partial \mathrm{NH_4}^{III}}{\partial t} = 0 = \frac{D_{\mathrm{NH_4}}}{1+K_{\mathrm{NH_4}}}\frac{\partial^2 \mathrm{NH_4}^{III}}{\partial z^2} - w\frac{\partial \mathrm{NH_4}^{III}}{\partial z} + \frac{1}{1+K_{\mathrm{NH_4}}}\cdot\frac{1-\phi}{\phi}\cdot\sum_i \mathrm{NC_i}\cdot k_i\cdot C_i(z) \tag{10}$$

The boundary conditions to solve Equations 6 - 10 are summarized in Table 3. The model assumes known bottom water concentrations for both species, the complete consumption of nitrate at the nitrate penetration depth (or zero flux if $z_{\mathrm{NO_3}} = z_{\infty}$) and no change in ammonium flux at $z_{\infty}$. It considers equal concentrations and diffusive fluxes at $z_{\mathrm{bio}}$ and $z_{\mathrm{ox}}$. In addition, the re-oxidation of upward-diffusing reduced ammonium is considered in the oxic-suboxic boundary condition for nitrate and ammonium.

### 2.3.4 Sulfate and Sulfide

When nitrate is depleted, sulfate reduction is the pathway to mineralize organic matter, thus consuming sulfate ($SO_4$) and producing hydrogen sulfide ($H_2S$) until the sulfate penetration depth ($z_{\mathrm{SO_4}}$).

**Table 3.** Boundary conditions for nitrate and ammonium.

| **Boundary** | **Condition** | |
|---|---|---|
| $z = 0$ | known concentration | 1) $NO_3(0) = NO_{30}$ |
| $z = z_{\mathrm{bio}}$ | continuity | 2) $NO_3(z_{\mathrm{bio}}^-)$=$NO_3(z_{\mathrm{bio}}^+)$ |
| | | 3) $-(D_{NO_3,0} + D_{\mathrm{bio}}) \cdot \frac{\partial NO_3}{\partial z}\vert_{z_{\mathrm{bio}}^-} = -D_{NO_3,0} \cdot \frac{\partial NO_3}{\partial z}\vert_{z_{\mathrm{bio}}^+}$ |
| $z = z_{\mathrm{ox}}$ | continuity | 4) $NO_3(z_{\mathrm{ox}}^-)$=$NO_3(z_{\mathrm{ox}}^+)$ |
| | | 5) $-D_{NO_3} \cdot \frac{\partial NO_3}{\partial z}\vert_{z_{\mathrm{ox}}^-} + \gamma_{\mathrm{NH_4}} \cdot F_{\mathrm{NH_4}}(z_{\mathrm{ox}}) = -D_{NO_3} \cdot \frac{\partial NO_3}{\partial z}\vert_{z_{\mathrm{ox}}^+}$ |
| | where: | $F_{\mathrm{NH_4}}(z_{\mathrm{ox}}) = \frac{1}{1+K_{\mathrm{NH_4}}} \cdot \frac{1-\phi}{\phi} \cdot \int_{z_{\mathrm{NO_3}}}^{\infty} \sum_i k_i \cdot \mathrm{NC_i} \cdot C_i \, dz$ |
| $z = z_{\mathrm{NO_3}}$ | $\mathrm{NO_3}$ consumption | 6) **IF** $(\mathrm{NO_3}(z_\infty) > 0)$ |
| | $(z_{\mathrm{NO_3}} = z_\infty)$ | $\frac{\partial NO_3}{\partial z}\vert_{z_{\mathrm{NO_3}}} = 0$ |
| | | **ELSE** |
| | $(z_{\mathrm{NO_3}} < z_\infty)$ | $NO_3(z_{\mathrm{NO_3}}) = 0$ |
| $z = 0$ | known concentration | 1) $\mathrm{NH_4}(0) = \mathrm{NH_{40}}$ |
| $z = z_{\mathrm{bio}}$ | continuity | 2) $\mathrm{NH_4}(z_{\mathrm{bio}}^-)$=$\mathrm{NH_4}(z_{\mathrm{bio}}^+)$ |
| | | 3) $-\frac{D_{\mathrm{NH_4},0}+D_{\mathrm{bio}}}{1+K_{\mathrm{NH_4}}} \cdot \frac{\partial \mathrm{NH_4}}{\partial z}\vert_{z_{\mathrm{bio}}^-} = -\frac{D_{\mathrm{NH_4},0}}{1+K_{\mathrm{NH_4}}} \cdot \frac{\partial \mathrm{NH_4}}{\partial z}\vert_{z_{\mathrm{bio}}^+}$ |
| $z = z_{\mathrm{ox}}$ | continuity | 4) $\mathrm{NH_4}(z_{\mathrm{ox}}^-)$=$\mathrm{NH_4}(z_{\mathrm{ox}}^+)$ |
| | | 5) $-\frac{D_{\mathrm{NH_4}}}{1+K_{\mathrm{NH_4}}} \cdot \frac{\partial \mathrm{NH_4}}{\partial z}\vert_{z_{\mathrm{ox}}^-} - \gamma_{\mathrm{NH_4}} \cdot F_{\mathrm{NH_4}}(z_{\mathrm{ox}}) = -\frac{D_{\mathrm{NH_4}}}{1+K_{\mathrm{NH_4}}} \cdot \frac{\partial \mathrm{NH_4}}{\partial z}\vert_{z_{\mathrm{ox}}^+}$ |
| | where: | $F_{\mathrm{NH_4}}(z_{\mathrm{ox}}) = \frac{1}{1+K_{\mathrm{NH_4}}} \cdot \frac{1-\phi}{\phi} \cdot \int_{z_{\mathrm{NO_3}}}^{\infty} \sum_i k_i \cdot \mathrm{NC_i} \cdot C_i \, dz$ |
| $z = z_{\mathrm{NO_3}}$ | continuity | 6) $\mathrm{NH_4}(z_{\mathrm{NO_3}}^-)$=$\mathrm{NH_4}(z_{\mathrm{NO_3}}^+)$ |
| | flux | 7) $-\frac{D_{\mathrm{NH_4}}}{1+K_{\mathrm{NH_4}}} \cdot \frac{\partial \mathrm{NH_4}}{\partial z}\vert_{z_{\mathrm{NO_3}}^-} = -\frac{D_{\mathrm{NH_4}}}{1+K_{\mathrm{NH_4}}} \cdot \frac{\partial \mathrm{NH_4}}{\partial z}\vert_{z_{\mathrm{NO_3}}^+}$ |
| $z = z_\infty$ | zero $\mathrm{NH_4}$ flux | 8) $\frac{\partial \mathrm{NH_4}}{\partial z}\vert_{z_\infty} = 0$ |

Sulfate and sulfide dynamics are thus described by:

1. Layer ($z \leq z_{\mathrm{NO_3}}$)

$$\frac{\partial \mathrm{SO_4}^I}{\partial t} = 0 = D_{\mathrm{SO_4}} \frac{\partial^2 \mathrm{SO_4}^I}{\partial z^2} - w \frac{\partial \mathrm{SO_4}^I}{\partial z} \tag{11}$$

$$\frac{\partial \mathrm{H_2S}^I}{\partial t} = 0 = D_{\mathrm{H_2S}} \frac{\partial^2 \mathrm{H_2S}^I}{\partial z^2} - w \frac{\partial \mathrm{H_2S}^I}{\partial z} \tag{12}$$

2. Layer ($z_{\mathrm{NO_3}} < z \leq z_{\mathrm{SO_4}}$)

$$\frac{\partial \mathrm{SO_4}^{II}}{\partial t} = 0 = D_{\mathrm{SO_4}} \frac{\partial^2 \mathrm{SO_4}^{II}}{\partial z^2} - w \frac{\partial \mathrm{SO_4}^{II}}{\partial z} - \frac{1-\phi}{\phi} \cdot \sum_i \mathrm{SO_4C} \cdot k_i \cdot C_i(z) \tag{13}$$

$$\frac{\partial \mathrm{H_2S}^{II}}{\partial t} = 0 = D_{\mathrm{H_2S}} \frac{\partial^2 \mathrm{H_2S}^{II}}{\partial z^2} - w \frac{\partial \mathrm{H_2S}^{II}}{\partial z} + \frac{1-\phi}{\phi} \cdot \sum_i \mathrm{SO_4C} \cdot k_i \cdot C_i(z) \tag{14}$$

3. Layer ($z_{\mathrm{SO_4}} < z \leq z_\infty$)

$$\frac{\partial \mathrm{H_2S}^{III}}{\partial t} = 0 = D_{\mathrm{H_2S}} \frac{\partial^2 \mathrm{H_2S}^{III}}{\partial z^2} - w \frac{\partial \mathrm{H_2S}^{III}}{\partial z} \tag{15}$$

**Table 4.** Boundary conditions for sulfate and sulfide.

| Boundary | Condition | | |
|---|---|---|---|
| $z = 0$ | known concentration | 1) | $SO_4(0)$=$SO_{40}$ |
| $z = z_{bio}$ | continuity | 2) | $SO_4(z^-_{bio})$=$SO_4(z^+_{bio})$ |
| | flux | 3) | $-(D_{SO_4,0} + D_{bio}) \cdot \frac{\partial SO_4}{\partial z}\|_{z^-_{bio}} = -D_{SO_4,0} \cdot \frac{\partial SO_4}{\partial z}\|_{z^+_{bio}}$ |
| $z = z_{ox}$ | continuity | 4) | $SO_4(z^-_{ox})$=$SO_4(z^+_{ox})$ |
| | flux | 5) | $-D_{SO_4} \cdot \frac{\partial SO_4}{\partial z}\|_{z^-_{ox}} + \gamma_{H_2S} \cdot F_{H_2S}(z_{ox}) = -D_{SO_4} \cdot \frac{\partial SO_4}{\partial z}\|_{z^+_{ox}}$ |
| | where: | | $F_{H_2S}(z_{ox}) = \frac{1-\phi}{\phi} \cdot \left( \int_{z_{NO_3}}^{SO_4} \sum_i SO_4C \cdot k_i \cdot C_i \, dz + \gamma_{CH_4} \cdot \int_{z_{SO_4}}^{\infty} \sum_i MC \cdot k_i \cdot C_i \, dz \right)$ |
| $z = z_{NO_3}$ | continuity | 6) | $SO_4(z^-_{NO_3})$=$SO_4(z^+_{NO_3})$ |
| | flux | 7) | $-D_{SO_4} \cdot \frac{\partial SO_4}{\partial z}\|_{z^-_{NO_3}} = -D_{SO_4} \cdot \frac{\partial SO_4}{\partial z}\|_{z^+_{NO_3}}$ |
| $z = z_{SO_4}$ | $SO_4$ consumption | 8) | **IF** $(SO_4(z_\infty) > 0)$ |
| | $(z_{SO_4} = z_\infty)$ | | $\frac{\partial SO_4}{\partial z}\|_{z_{SO_4}} = 0$ |
| | | | **ELSE** |
| | $(z_{SO_4} < z_\infty)$ | | $SO_4(z_{SO_4}) = 0$ and $-D_{SO_4} \cdot \frac{\partial SO_4}{\partial z}\|_{z_{SO_4}} = \gamma_{CH_4} \cdot F_{CH_4}(z_{SO_4})$ |
| | with flux from below: | | $F_{CH_4}(z_{SO_4}) = \frac{1-\phi}{\phi} \cdot \int_{z_{SO_4}}^{\infty} \sum_i MC \cdot k_i \cdot C_i \, dz$ |
| $z = 0$ | known concentration | 1) | $H_2S(0) = H_2S_0$ |
| $z = z_{bio}$ | continuity | 2) | $H_2S(z^-_{bio})$=$H_2S(z^+_{bio})$ |
| | flux | 3) | $-(D_{H_2S,0} + D_{bio}) \cdot \frac{\partial H_2S}{\partial z}\|_{z^-_{bio}} = -D_{H_2S,0} \cdot \frac{\partial H_2S}{\partial z}\|_{z^+_{bio}}$ |
| $z = z_{ox}$ | continuity | 4) | $H_2S(z^-_{ox})$=$H_2S(z^+_{ox})$ |
| | flux | 5) | $-D_{H_2S} \cdot \frac{\partial H_2S}{\partial z}\|_{z^-_{ox}} - \gamma_{H_2S} F_{H_2S}(z_{ox}) = -D_{H_2S} \cdot \frac{\partial H_2S}{\partial z}\|_{z^+_{ox}}$ |
| | where: | | $F_{H_2S}(z_{ox}) = \frac{1-\phi}{\phi} \cdot \left( \int_{z_{NO_3}}^{SO_4} \sum_i SO_4C \cdot k_i \cdot C_i \, dz + \gamma_{CH_4} \cdot \int_{z_{SO_4}}^{\infty} \sum_i MC \cdot k_i \cdot C_i \, dz \right)$ |
| $z = z_{NO_3}$ | continuity | 6) | $H_2S(z^-_{NO_3})$=$H_2S(z^+_{NO_3})$ |
| | flux | 7) | $-D_{H_2S} \cdot \frac{\partial H_2S}{\partial z}\|_{z^-_{NO_3}} = -D_{H_2S} \cdot \frac{\partial H_2S}{\partial z}\|_{z^+_{NO_3}}$ |
| $z = z_{SO_4}$ | continuity | 8) | $H_2S(z^-_{SO_4})$=$H_2S(z^+_{SO_4})$ |
| | flux (with AOM) | 9) | $-D_{H_2S} \cdot \frac{\partial H_2S}{\partial z}\|_{z^-_{SO_4}} + \gamma_{CH_4} \cdot F_{CH_4}(z_{SO_4}) = -D_{H_2S} \cdot \frac{\partial H_2S}{\partial z}\|_{z^+_{SO_4}}$ |
| | where: | | $F_{CH_4}(z_{SO_4}) = \frac{1-\phi}{\phi} \cdot \int_{z_{SO_4}}^{\infty} \sum_i MC \cdot k_i \cdot C_i \, dz$ |
| $z = z_\infty$ | zero $H_2S$ flux | 10) | $\frac{\partial H_2S}{\partial z}\|_{z_\infty} = 0$ |

DH: @Sandra: BC 5) Include $\int_{z_{SO_4}}^{\infty}$ here?

DH: @Sandra: think yes, because at 8) $CH_4$ from $\int_{z_{SO_4}}^{\infty}$ is oxidised to $H_2S$; at 5) this $H_2S$ to $SO_4$

To solve equations 11 - 15 the model assumes known concentrations at the sediment-water interface and continuity across the bioturbation depth and the nitrate penetration depth (see Table 4). The re-oxidation of reduced $H_2S$ to $SO_4$ is considered in the oxic-suboxic boundary condition for both species, here including the methanic zone, as $H_2S$ is also produced during anaerobic oxidation of methane (AOM). Furthermore, sulfate is used at $z_{SO_4}$ to oxidize methane from below and thus producing $H_2S$. In case $z_{SO_4} < z_\infty$, sulfate concentration is zero at $z_{SO_4}$ and its diffusive flux must equal the amount of methane produced below; or, in case $z_{SO_4} = z_\infty$, a zero flux condition for sulfate is considered. At lower boundary ($z_\infty$) zero flux of $H_2S$ is considered. correct??

### 2.3.5 Phosphate

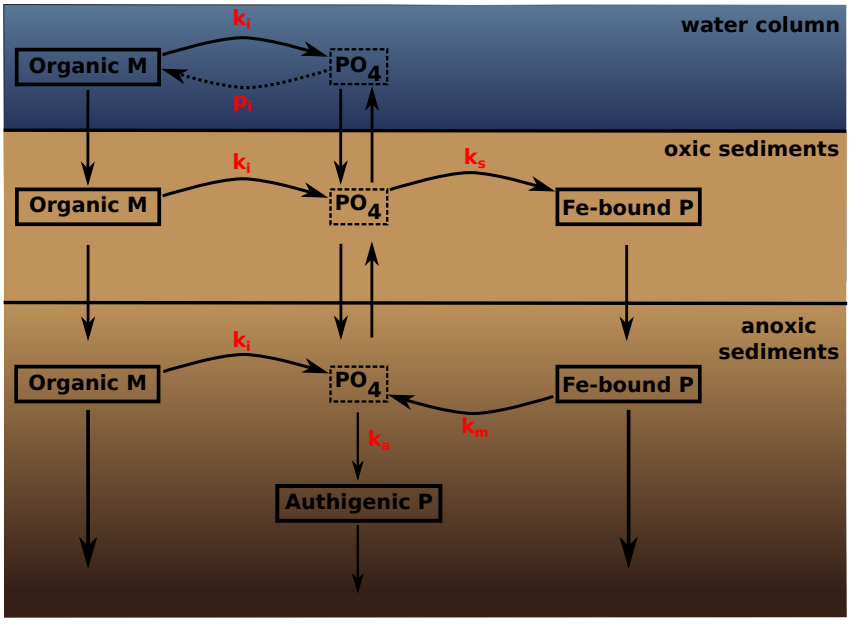


**Figure 2.** A schematic of the sedimentary P cycle in OMEN-SED (1.0). Red numbers represent kinetic rate constants for phosphorus dynamics (compare Table 7; $p_i$ represents uptake rate of $PO_4$ via primary production in shallow environments). Adapted from Slomp et al. (1996).

To model phosphorus (P) in the sediments the model takes into account the change with depth of phosphate ($PO_4$) and iron-bound P, thereby mainly following the description of Slomp et al. (1996) and Gypens et al. (2008). Throughout the sediment column organic matter is mineralized resulting in a release of phosphate to the pore water. In the oxic part of the sediment, this $PO_4$ either diffuses upward to the water column or is adsorped to Fe oxides forming Fe-bound P (or M)(Slomp et al., 1998). In the suboxic/anoxic zone, $PO_4$ is not only produced through organic matter degradation but is also released from the Fe-bound P pool due to the reduction of Fe oxides. Furthermore, phosphate concentrations can become high enough in this layer for authigenic mineral formation to occur (Cappellen and Berner, 1988). This phosphorus bound in authigenic minerals represents a permanent sink for reactive phosphorus (Slomp et al., 1996). See Figure 2 for a schematic overview of the sedimentary P cycle. Therefore the diagenetic equations for phosphorus are written:

**Table 5.** Boundary conditions for phosphate and Fe-bound P (M).

| **Boundary** | **Condition** | |
|---|---|---|
| $z = 0$ | known concentration | 1) $\mathrm{PO_4}(0)=\mathrm{PO_{40}}$ |
| $z = z_{\mathrm{bio}}$ | continuity | 2) $\mathrm{PO_4}(z_{\mathrm{bio}}^-)=\mathrm{PO_4}(z_{\mathrm{bio}}^+)$ |
| | flux | 3) $(D_{\mathrm{PO_4},0} + D_{\mathrm{bio}}) \cdot \frac{\partial \mathrm{PO_4}}{\partial z}\vert_{z_{\mathrm{bio}}^-} = D_{\mathrm{PO_4},0} \cdot \frac{\partial \mathrm{PO_4}}{\partial z}\vert_{z_{\mathrm{bio}}^+}$ |
| $z = z_{\mathrm{ox}}$ | continuity | 4) $\mathrm{PO_4}(z_{\mathrm{ox}}^-)=\mathrm{PO_4}(z_{\mathrm{ox}}^+)$ |
| | flux | 5) $-\frac{D_{\mathrm{PO_4}}}{1+K_{\mathrm{PO_4}}^I} \cdot \frac{\partial \mathrm{PO_4}}{\partial z}\vert_{z_{\mathrm{ox}}^-} = -\frac{D_{\mathrm{PO_4}}}{1+K_{\mathrm{PO_4}}^{II}} \cdot \frac{\partial \mathrm{PO_4}}{\partial z}\vert_{z_{\mathrm{ox}}^+}$ |
| $z = z_{\infty}$ | flux | 10) $\frac{\partial \mathrm{PO_4}}{\partial z}\vert_{z_\infty} = 0$ |
| $z = 0$ | known concentration | 1) $M(0) = M_0$ |
| $z = z_{\mathrm{bio}}$ | continuity | 2) $M(z_{\mathrm{bio}}^-)=M(z_{\mathrm{bio}}^+)$ |
| | flux | 3) $\frac{\partial M}{\partial z}\vert_{z_{\mathrm{bio}}^-} = \frac{\partial M}{\partial z}\vert_{z_{\mathrm{bio}}^+}$ |
| $z = z_{\mathrm{ox}}$ | continuity | 4) $M(z_{\mathrm{ox}}^-)=M(z_{\mathrm{ox}}^+)$ |
| | flux | 5) $\frac{\partial M}{\partial z}\vert_{z_{\mathrm{ox}}^-} = \frac{\partial M}{\partial z}\vert_{z_{\mathrm{ox}}^+}$ |
| $z = z_{\infty}$ | assymptotic concentration | 10) $M(z_\infty) = M_\infty$ |

1. Layer ($z \leq z_{\mathrm{ox}}$)

$$\frac{\partial \mathrm{PO_4}^I}{\partial t} = \frac{D_{\mathrm{PO_4}}}{1+K_{\mathrm{PO_4}}^I}\frac{\partial^2 \mathrm{PO_4}^I}{\partial z^2} - w\frac{\partial \mathrm{PO_4}^I}{\partial z} + \frac{1-\phi}{\phi}\frac{1}{1+K_{\mathrm{PO_4}}^I}\sum_i(\mathrm{PC}_i \cdot k_i \cdot C_i(z)) - \frac{k_s}{1+K_{\mathrm{PO_4}}^I}(\mathrm{PO_4}^I - \mathrm{PO_4}^s) \tag{16}$$

$$\frac{\partial M^I}{\partial t} = D_M\frac{\partial^2 M^I}{\partial z^2} - w\frac{\partial M^I}{\partial z} + \frac{\phi}{1-\phi}k_s(\mathrm{PO_4}^I - \mathrm{PO_4}^s) \tag{17}$$

2. Layer ($z_{\mathrm{ox}} < z$)

$$\frac{\partial M^{II}}{\partial t} = D_M\frac{\partial^2 M^{II}}{\partial z^2} - w\frac{\partial M^{II}}{\partial z} - k_m(M^{II} - M^\infty) \tag{18}$$

$$\frac{\partial \mathrm{PO_4}^{II}}{\partial t} = \frac{D_{\mathrm{PO_4}}}{1+K_{\mathrm{PO_4}}^{II}}\frac{\partial^2 \mathrm{PO_4}^{II}}{\partial z^2} - w\frac{\partial \mathrm{PO_4}^{II}}{\partial z} + \frac{1-\phi}{\phi}\frac{1}{1+K_{\mathrm{PO_4}}^{II}}\sum_i(\mathrm{PC}_i \cdot k_i \cdot C_i(z)) - \frac{k_a}{1+K_{\mathrm{PO_4}}^{II}}(\mathrm{PO_4}^{II} - \mathrm{PO_4}^a) + \frac{(1-\phi)}{\phi}\frac{k_m}{1+K_{\mathrm{PO_4}}^{II}}(M^{II} - M^\infty) \tag{19}$$

$$\tag{20}$$

The boundary conditions to solve Equations 16 - 19 are summarized in Table 5. The model assumes known bottom water concentrations and equal concentrations and diffusive fluxes at $z_{\mathrm{bio}}$ and $z_{\mathrm{ox}}$ for both species. Additionally it considers no change in phosphate flux and an assymptotic Fe-bound P concentration at $z_\infty$.

@ Sandra: SWI Flux for M does not exist, right???

### 2.3.6 Dissolved Inorganic Carbon (DIC)

### 2.3.7 Alkalinity

## 2.4 Model Parameters

This section describes the parameters used in OMEN-SED (1.0) to describe sediment transport and biogeochemical reactions related to the burial and mineralization of organic matter under a wide range of environmental conditions. Table 6 states the parameters for sediment characteristics and Table 7 summarizes the stoichiometric factors and secondary reaction parameters used in the model.

### 2.4.1 Transport Parameters

Advection is the bulk flow of sediments and can be directly related to the accumulation of new material on the seafloor (i.e. sedimentation, Burdige, 2006). This results in a downward flux of older sediment material and porewater in relation to the sediment-water interface. OMEN-SED (1.0) uses the empirical global relationship between sediment accumulation rate (cm $yr^{-1}$) and seafloor depth (m) of Middelburg et al. (1997):

$$w = 3.3 \cdot 10^{-0.87478367 - 0.00043512 \cdot \text{depth}} \tag{21}$$

As discussed before (Sec. 2.2), the diffusion coefficient of species $i$ is calculated as $D_i = D_{i,0} + D_{\text{bio}} = D_{\text{mol},i} \cdot f_{ir} + D_{\text{bio}}$ for dissolved species and $D_i = D_{\text{bio}}$ for solid species. The bioturbation coefficient $D_{\text{bio}}$ ($cm^2$ $yr^-1$) is constant in the bioturbated zone and also follows the empirical relationship by Middelburg et al. (1997):

$$D_{\text{bio}} = 5.2 \cdot 10^{0.76241122 - 0.00039724 \cdot \text{depth}} \tag{22}$$

Studies showed that bioturbational effects on a global scale are largely restricted to the upper 10 cm of the sediments and are only marginally related to seafloor depth (e.g. Boudreau, 1998; Teal et al., 2010). Therefore, OMEN-SED (1.0) imposes a globally invariant bioturbation depth of 10 cm. Bioirrigation can enhance the molecular diffusion coefficient $D_{i,0} = D_{\text{mol},i} \cdot f_{ir}$ (Soetaert et al., 1996a). However, here we do not consider this effect and set $f_{ir}$ to a constant value of 1. The specific molecular diffusion coefficients $D_{\text{mol},i}$ are corrected for sediment porosity $\phi$, tortuosity F and are linearly interpolated for an ambient temperature $T$ using zero-degree coefficients $D_i^0$ and temperature dependent diffusion coefficients $D_i^T$ (compare Gypens et al., 2008):

$$D_{\text{mol},i} = (D_i^0 + D_i^T \cdot T) \cdot \frac{1}{\phi \cdot F}$$

Tortuosity can be expresssed in terms of porosity as $F = \frac{1}{\phi^m}$ (Ullman and Aller, 1982) with the exponent $m$ varying according to the type of sediment (here we use m=3). Values for $D_i^T$ and $D_i^0$ are summarized in Table 6 and are adapted from Li and Gregory (1974) and Gypens et al. (2008).

**Table 6.** Fixed sediment characteristics and transport parameters. TODO: Update table!

| Parameter | Unit | Value | Description/Source |
|---|---|---|---|
| $\rho_{\text{sed}}$ | $\text{g}\,\text{cm}^{-3}$ | 2.5 | Sediment density |
| $w$ | $\text{cm}\,\text{yr}^{-1}$ | Fct. of seafloor | Advection/Sediment accumulation rate |
| | | depth | Middelburg et al. (1997) |
| $z_{\text{bio}}$ | cm | 10 | Bioturbation depth |
| | | | Boudreau (1998); Teal et al. (2010) |
| $D_{\text{bio}}$ | $\text{cm}^2\,\text{yr}^{-1}$ | Fct. of seafloor | Bioturbation coefficient |
| | | depth | Middelburg et al. (1997) |
| $\phi$ | - | 0.8 | Porosity |
| F | - | $\frac{1}{\phi^m}$ | Tortuosity, here m=3 |
| $\text{f}_{ir}$ | - | 1 | Irrigation factor |
| $\text{PO}_4{}^s$ | $\text{mol}\,\text{cm}^{-3}$ | $1 \cdot 10^{-9}$ | equilibrium conc. for P sorption |
| | | | Slomp et al. (1996) |
| $\text{PO}_4{}^a$ | $\text{mol}\,\text{cm}^{-3}$ | $3.7 \cdot 10^{-9}$ | equilibrium conc. for authigenic P precipitation |
| | | | Slomp et al. (1996) |
| $\text{M}^\infty$ | $\text{mol}\,\text{cm}^{-3}$ | $1.99 \cdot 10^{-9}$ | asymptotic concentration for Fe-bound P |
| | | | Slomp et al. (1996) |
| **Diffusion coefficients** (Li and Gregory, 1974; Gypens et al., 2008) | | | |
| $D^0_{\text{O}_2}$ | $\text{cm}^2\,\text{yr}^{-1}$ | 348.62172 | Molecular diffusion coefficient of oxygen at 0°C |
| $D^T_{\text{O}_2}$ | $\text{cm}^2\,\text{yr}^{-1}\,^\circ\text{C}^{-1}$ | 14.08608 | Diffusion coefficient for linear temp. dependence of oxygen |
| $D^0_{\text{NO}_3}$ | $\text{cm}^2\,\text{yr}^{-1}$ | 308.42208 | Molecular diffusion coefficient of nitrate at 0°C |
| $D^T_{\text{NO}_3}$ | $\text{cm}^2\,\text{yr}^{-1}\,^\circ\text{C}^{-1}$ | 12.2640 | Diffusion coefficient for linear temp. dependence of nitrate |
| $D^0_{\text{NH}_4}$ | $\text{cm}^2\,\text{yr}^{-1}$ | 308.42208 | Molecular diffusion coefficient of ammonium at 0°C |
| $D^T_{\text{NH}_4}$ | $\text{cm}^2\,\text{yr}^{-1}\,^\circ\text{C}^{-1}$ | 12.2640 | Diffusion coefficient for linear temp. dependence of ammonium |
| $D^0_{\text{SO}_4}$ | $\text{cm}^2\,\text{yr}^{-1}$ | 157.68 | Molecular diffusion coefficient of sulfate at 0°C |
| $D^T_{\text{SO}_4}$ | $\text{cm}^2\,\text{yr}^{-1}\,^\circ\text{C}^{-1}$ | 7.884 | Diffusion coefficient for linear temp. dependence of sulfate |
| $D^0_{\text{H}_2\text{S}}$ | $\text{cm}^2\,\text{yr}^{-1}$ | 307.476 | Molecular diffusion coefficient of sulfide at 0°C |
| $D^T_{\text{H}_2\text{S}}$ | $\text{cm}^2\,\text{yr}^{-1}\,^\circ\text{C}^{-1}$ | 9.636 | Diffusion coefficient for linear temp. dependence of sulfide |
| $D^0_{\text{PO}_4}$ | $\text{cm}^2\,\text{yr}^{-1}$ | 112.90764 | Molecular diffusion coefficient of phosphate at 0°C |
| $D^T_{\text{PO}_4}$ | $\text{cm}^2\,\text{yr}^{-1}\,^\circ\text{C}^{-1}$ | 5.586252 | Diffusion coefficient for linear temp. dependence of phosphate |

**Table 7.** Values for biogeochemical parameters used in OMEN-SED (1.0).

| Parameter/Variable | Unit | Value | Description |
|---|---|---|---|
| **Stoichiometric factors and molecular ratios** | | | |
| $NC_1$ | mol/mol | 0.1509 | nitrogen to carbon ratio |
| | | | refractory fraction, two different ones? why these values? |
| $NC_2$ | mol/mol | 0.13333 | nitrogen to carbon ratio |
| | | | labile fraction |
| $PC_i$ | mol/mol | 0.0094 | phosphorus to carbon ratio |
| $MC$ | mol/mol | 0.5 | methane to carbon ratio |
| | | | produced during methanogenesis |
| $OC$ | mol/mol | 1.0 | oxygen to carbon ratio |
| $NO_3C$ | mol/mol | 94.4/106 | nitrate to carbon ratio |
| $SO_4C$ | mol/mol | 0.5 | sulfate to carbon ratio |
| **Secondary reaction parameters** | | | |
| $\gamma_{NH_4}$ | - | 1.0 | fraction of $NH_4$ that is oxidised |
| | | | in oxic layer |
| $\gamma_{H_2S}$ | - | 0.8 | fraction of $H_2S$ that is oxidised |
| | | | in oxic layer |
| $\gamma_{CH_4}$ | - | 1.0 | fraction of $CH_4$ that is oxidised |
| | | | at $z_{SO_4}$ |
| **Rate constants** | | | |
| $k_i$ | $yr^{-1}$ | from Earth System Model | OM degradation rate constants |
| $k_s$ | $yr^{-1}$ | ??? | rate constant for P sorption |
| $k_m$ | $yr^{-1}$ | ??? | rate constant for Fe-bound P release |
| $k_a$ | $yr^{-1}$ | ??? | rate constant for authigenic P formation |

### 2.4.2 Reaction Parameters

The applied multi-G approach for organic matter degradation considers specific degradation rate constants $k_i$ ($yr^{-1}$) for each compound class. The degradation constants are generally taken from the coupled Earth System model and are assumed invariant along the sediment column, therefore independent of the nature of the terminal electron acceptor. The stoichiometry of organic matter is represented by the factors $NC_i$ and $PC_i$ denoting the molecular nitrogen to carbon and phosphorus to carbon ratio. In the sulfidic and methanic zone the reduction of 1 mol organic matter additionally produces 0.5 mol of hydrogen sulfide ($SO_4C$) and 0.5 mol of methane ($MC$). In the total sediment column organic matter mineralization consumes the specific terminal electron acceptor with a fixed ratio ($OC$, $NO_3C$ and $SO_4C$ respectively). See Table 7 for a complete summary of the parameters and their values.

### 2.5 Module Structure

TODO: An analytical steady-state solution is found for the reaction-transport equation of each chemical species in each layer. At each boundary (i.e. $z_{\mathrm{ox}}, z_{\mathrm{bio}}, z_{\mathrm{NO_3}}$ and $z_{\mathrm{SO_4}}$) the model has to match continuity and flux for different ODE solutions of the layer above and below the specific boundary. In particular the bioturbation boundary is problematic as it can theoretically occur in any geochemical layer. In order to simplify this recurring boundary matching problem it is implemented in an independent algorithm which is described in Section 2.5.1. Instructions and requirements for coupling OMEN-SED (1.0) to a global Earth Sytem Model are given in Section 2.5.2.

#### 2.5.1 Generic boundary condition matching (GBCM)

A general steady-state advection-diffusion-reaction (ADR) diagenetic equation looks like:

$$\frac{\partial C}{\partial t} = 0 = D\frac{\partial^2 C}{\partial z^2} - w\frac{\partial C}{\partial z} - \sum_i \alpha_i \exp(-\beta_i z) - k \cdot C + Q. \tag{23}$$

where $z$ is the sediment depth, $t$ the time, $D$ is the diffusion coefficient and $w$ is the advection rate. The ODE solution is of the general form:

$$C(z) = A\exp(az) + B\exp(bz) + \sum_i \frac{\alpha_i}{D\beta_i^2 - w\beta_i - k} \cdot \exp(-\beta_i z) + \frac{Q}{k} \tag{24}$$

and can therefore be expressed as:

$$C(z) = A \cdot E(z) + B \cdot F(z) + G(z) \tag{25}$$

where $E(z)$, $F(z)$ are the homogeneous solutions of the ODE, G(z) the particular integral, and A, B are the integration constants.

Each boundary matching problem involves matching continuity and flux for the two solutions $C_U(z)$ (= 'upper') and $C_L(z)$ (= 'lower') across a boundary at $z = z_b$. Therefore, we get two ODE solutions of the genral form:

$$C_U(z) = A_U \cdot E_U(z) + B_U \cdot F_U(z) + G_U(z) \tag{26}$$

$$C_L(z) = A_L \cdot E_L(z) + B_L \cdot F_L(z) + G_L(z). \tag{27}$$

The two boundary conditions are: for continuity (where for generality we allow a discontinuity $V_b$)

$$C_U(z_b) = C_L(z_b) + V_b \tag{28}$$

and for flux

$$D_U C'_U(z_b) + wC_U(z_b) = D_L C'_L(z_b) + wC_L(z_b) + F_b \tag{29}$$

where $w$ is advection, $D$ are the diffusion coefficients and $F_b$ is any flux discontinuity.

In terms of the ODE solutions (26), (27), the boundary conditions represent two equations connecting the four integration constants:

$$\begin{pmatrix} E_U & F_U \\ D_U E'_U & D_U F'_U \end{pmatrix} \begin{pmatrix} A_U \\ B_U \end{pmatrix} = \begin{pmatrix} E_L & F_L \\ D_L E'_L & D_L F'_L \end{pmatrix} \begin{pmatrix} A_L \\ B_L \end{pmatrix} + \begin{pmatrix} G_L - G_U + V_b \\ D_L G'_L - D_U G'_U + F_b - w V_b \end{pmatrix} \tag{30}$$

where the ODE solutions $E,\ F,\ G$ are all evaluated at $z_b$.

Equation (30) can be solved to give $A_U$ and $B_U$ as a function of the integration constants from the layer below ($A_L$ and $B_L$), thereby constructing a piecewise solution for the whole region, with now just two integration constants $A_L$ and $B_L$.

In the code the function **benthic_utils.matchsoln** provides this solution in the form:

$$\begin{pmatrix} A_U \\ B_U \end{pmatrix} = \begin{pmatrix} c_1 & c_2 \\ c_3 & c_4 \end{pmatrix} \begin{pmatrix} A_L \\ B_L \end{pmatrix} + \begin{pmatrix} d_1 \\ d_2 \end{pmatrix}. \tag{31}$$

Using (31) we can now rewrite $C_U(z)$ in (26) as a function of $A_L$ and $B_L$:

$$C_U(z) = (c_1 A_L + c_2 B_L + d_1) \cdot E_U(z) + (c_3 A_L + c_4 B_L + d_2) \cdot F_U(z) + G_U(z)$$

and hence define the "transformed" basis functions $E^*_U(z),\ F^*_U(z),\ G^*_U(z)$ such that:

$$C_U(z) = A_L \cdot E^*_U(z) + B_L \cdot F^*_U(z) + G^*_U(z) \tag{32}$$

where

$$\begin{aligned} E^*_U(z) &= c_1 E_U(z) + c_3 F_U(z) \\ F^*_U(z) &= c_2 E_U(z) + c_4 F_U(z) \\ G^*_U(z) &= G_U(z) + d_1 E_U(z) + d_2 F_U(z) \end{aligned} \tag{33}$$

(in the code this is done by **benthic_utils.xformsoln**).

**Solving the sediment layer stack**

Equations (31), (32) and (33) can now be applied for each layer boundary, working up from the bottom of the sediments. The net result is to construct a piecewise solution with just two integration constants (coming from the lowest layer), which can then be solved for by applying one boundary condition for the sediment-water interface and one for the bottom of the sediments (e.g. a concentration condition at the bottom of the sediments, and a flux condition at the SWI).

**TODO: Add figure, illustrating this e.g. for nitrate...**

**Abstracting out the bioturbation boundary**

The bioturbation boundary affects the diffusion coefficient of the modelled solutes and the conservation equation of organic matter which is available for mineralization. The boundary is particularly inconvenient as it can in principle occur in the middle of any "geochemical" layer and therefore generates multiple cases. To simplify this for solutes, the "piecewise solution construction" above is used to abstract out the bioturbation boundary. An initial test for each layer is made to identify its "bioturbation-status" (fully bioturbated, fully non-bioturbated or crossing the bioturbation boundary) and (if needed) a piecewise solution is constructed by matching boundary conditions across the bioturbation boundary. The "outside" code therefore never needs to know whether it is dealing with a piecewise solution (i.e. matched across a bioturbation boundary) or a "simple" solution (i.e. the layer is fully bioturbated or fully non-bioturbated).

In the code, this is performed by **zTOC.prepfg_l12** which hands back a structure ls containing the "bioturbation-status" for each layer and (if needed) the description of the piecewise solution (coeffcients $c_1, c_2, c_3, c_4, d_1, d_2$ as above). So e.g. for sulfate, **zTOC.prepfg_l12** is called three times at the beginning of **zSO4.calcbc** (one for each "geochemical" layer: oxic, suboxic, sulfidic) handing back three structures ls describing the layer's "bioturbation-status", abstracting away the bioturbation boundary and all associated conditional logic. When calculating the solutions for the different layers, the pre-calculated structure ls is passed to the function **zTOC.calcfg_l12** which sorts out the correct solution type to use.

### 2.5.2 Coupling to an Earth System Model

## 3 Test Cases

### 3.1 Benthic fluxes on a global scale

Application to Seitert, 2004 OM, burwiczk see rate data and evaluation based on global data (Archer)

### 3.2 HILDA-like test

### 3.3 GENIE-Cretaceous test?

## 4 Scope of applicability and model limitations

## 5 Conclusions

TEXT

## 6 Code Availability

## Appendix A

### A1

*Acknowledgements.* TEXT

## References


Aguilera, D. R., Jourabchi, P., Spiteri, C., and Regnier, P. (2005). A knowledge-based reactive transport approach for the simulation of biogeochemical dynamics in Earth systems. *Geochemistry, Geophysics, Geosystems*, 6(7):Q07012. 00046.

Arndt, S., Jørgensen, B., LaRowe, D., Middelburg, J., Pancost, R., and Regnier, P. (2013). Quantifying the degradation of organic matter in marine sediments: A review and synthesis. *Earth-Science Reviews*, 123:53–86.

Berner, R. A. (1980). *Early Diagenesis: A Theoretical Approach*. Princeton University Press.

Berner, R. A. (2004). *The Phanerozoic Carbon Cycle: CO2 and O2*. Oxford University Press. 00000.

Billen, G. (1982). Modelling the processes of organic matter degradation and nutrients recycling in sedimentary systems. *Sediment microbiology*, pages 15–52.

Boudreau, B. P. (1997). *Diagenetic models and their implementation*, volume 505. Springer Berlin.

Boudreau, B. P. (1998). Mean mixed depth of sediments: The wherefore and the why. *Limnology and Oceanography*, 43(3):524–526.

Burdige, D. J. (2006). *Geochemistry of marine sediments*, volume 398. Princeton University Press Princeton.

Burdige, D. J. (2007). Preservation of Organic Matter in Marine Sediments: Controls, Mechanisms, and an Imbalance in Sediment Organic Carbon Budgets? *Chemical Reviews*, 107(2):467–485.

Cappellen, P. V. and Berner, R. A. (1988). A mathematical model for the early diagenesis of phosphorus and fluorine in marine sediments; apatite precipitation. *American Journal of Science*, 288(4):289–333.

Goloway, F. and Bender, M. (1982). Diagenetic models of interstitial nitrate profiles in deep sea suboxic sediments. *Limnol. Oceanogr*, 27(4):624–638.

Goosse, H., Brovkin, V., Fichefet, T., Haarsma, R., Huybrechts, P., Jongma, J., Mouchet, A., Selten, F., Barriat, P.-Y., Campin, J.-M., Deleersnijder, E., Driesschaert, E., Goelzer, H., Janssens, I., Loutre, M.-F., Morales Maqueda, M. A., Opsteegh, T., Mathieu, P.-P., Munhoven, G., Pettersson, E. J., Renssen, H., Roche, D. M., Schaeffer, M., Tartinville, B., Timmermann, A., and Weber, S. L. (2010). Description of the earth system model of intermediate complexity LOVECLIM version 1.2. *Geosci. Model Dev.*, 3(2):603–633.

Gypens, N., Lancelot, C., and Soetaert, K. (2008). Simple parameterisations for describing n and p diagenetic processes: Application in the north sea. *Progress in Oceanography*, 76(1):89–110.

Heinze, C., Maier-Reimer, E., Winguth, A. M. E., and Archer, D. (1999). A global oceanic sediment model for long-term climate studies. *Global Biogeochemical Cycles*, 13(1):221–250.

Hülse, D., Arndt, S., Wilson, J., Munhoven, G., and Ridgwell, A. (2016). The biological carbon pump in paleoclimate models: A model review. *Earth-Science Reviews*, –:in review.

Jahnke, R. A., Emerson, S. R., and Murray, J. W. (1982). A model of oxygen reduction, denitrification, and organic matter mineralization in marine sediments. *Limnol. Oceanogr*, 27(4):6–10.

Kriest, I. and Oschlies, A. (2011). Numerical effects on organic-matter sedimentation and remineralization in biogeochemical ocean models. *Ocean Modelling*, 39(3–4):275–283.

Li, Y.-H. and Gregory, S. (1974). Diffusion of ions in sea water and in deep-sea sediments. *Geochimica et Cosmochimica Acta*, 38(5):703–714.

Mackenzie, F. T. (2005). *Sediments, Diagenesis, and Sedimentary Rocks: Treatise on Geochemistry, Second Edition*. Elsevier. 00000.

Mackenzie, F. T., Lerman, A., and Andersson, A. J. (2004). Past and present of sediment and carbon biogeochemical cycling models. *Biogeosciences*, 1(1):11–32.

Meysman, F. J. R., Middelburg, J. J., Herman, P. M. J., and Heip, C. H. R. (2003). Reactive transport in surface sediments. II. Media: an object-oriented problem-solving environment for early diagenesis. *Computers & Geosciences*, 29(3):301–318. 00067.

Middelburg, J. J., Soetaert, K., and Herman, P. M. (1997). Empirical relationships for use in global diagenetic models. *Deep Sea Research Part I: Oceanographic Research Papers*, 44(2):327–344.

Munhoven, G. (2007). Glacial–interglacial rain ratio changes: Implications for atmospheric and ocean–sediment interaction. *Deep Sea Research Part II: Topical Studies in Oceanography*, 54(5–7):722–746.

Najjar, R. G., Jin, X., Louanchi, F., Aumont, O., Caldeira, K., Doney, S. C., Dutay, J.-C., Follows, M., Gruber, N., Joos, F., Lindsay, K., Maier-Reimer, E., Matear, R. J., Matsumoto, K., Monfray, P., Mouchet, A., Orr, J. C., Plattner, G.-K., Sarmiento, J. L., Schlitzer, R., Slater, R. D., Weirig, M.-F., Yamanaka, Y., and Yool, A. (2007). Impact of circulation on export production, dissolved organic matter, and dissolved oxygen in the ocean: Results from Phase II of the Ocean Carbon-cycle Model Intercomparison Project (OCMIP-2). *Global Biogeochemical Cycles*, 21(3):GB3007.

Ridgwell, A., Hargreaves, J. C., Edwards, N. R., Annan, J. D., Lenton, T. M., Marsh, R., Yool, A., and Watson, A. (2007). Marine geochemical data assimilation in an efficient Earth System Model of global biogeochemical cycling. *Biogeosciences*, 4(1):87–104. 00090.

Shaffer, G., Malskær Olsen, S., and Pepke Pedersen, J. O. (2008). Presentation, calibration and validation of the low-order, DCESS Earth System Model (Version 1). *Geosci. Model Dev.*, 1(1):17–51. 00007.

Slomp, C., Malschaert, J., and Van Raaphorst, W. (1998). The role of adsorption in sediment-water exchange of phosphate in north sea continental margin sediments. *Limnology and Oceanography*, 43(5):832–846.

Slomp, C. P., Epping, E. H., Helder, W., and Van Raaphorst, W. (1996). A key role for iron-bound phosphorus in authigenic apatite formation in north atlantic continental platform sediments. *Journal of Marine Research*, 54(6):1179–1205.

Soetaert, K., Herman, P. M., and Middelburg, J. J. (1996a). Dynamic response of deep-sea sediments to seasonal variations: a model. *Limnology and Oceanography*, 41(8):1651–1668.

Soetaert, K., Herman, P. M. J., and Middelburg, J. J. (1996b). A model of early diagenetic processes from the shelf to abyssal depths. *Geochimica et Cosmochimica Acta*, 60(6):1019–1040.

Soetaert, K., Middelburg, J. J., Herman, P. M. J., and Buis, K. (2000). On the coupling of benthic and pelagic biogeochemical models. *Earth-Science Reviews*, 51(1–4):173–201.

Teal, L., Bulling, M., Parker, E., and Solan, M. (2010). Global patterns of bioturbation intensity and mixed depth of marine soft sediments. *Aquatic Biology*, 2(3):207–218.

Ullman, W. J. and Aller, R. C. (1982). Diffusion coefficients in nearshore marine sediments. *Limnology and Oceanography*, 27(3):552–556.